Given the Bond albedo and an estimate of the surface temperature, T, the emissivity of Triton can be determined from the energy balance equation

$$(1 - A_B)F_\odot = 4\epsilon\sigma T^4 \quad (11)$$

where $F_\odot$ is the integrated solar flux, σ is the Stefan-Boltzmann constant, and ϵ is the emissivity. Assuming a 14-μbar N_2 atmosphere in vapor equilibrium everywhere with an N_2-covered surface (therefore implying a uniform surface temperature of ~37.5 K), our Bond albedo yields a surface emissivity of 0.59 ± 0.16. The error quoted does not include possible errors in the temperature.

Our value of 0.59 for Triton's emissivity is unusually low. In comparison, almost all other satellites exhibit much higher emissivities, typically ~0.9 (*19*). A low emissivity for Triton may not be unreasonable: Triton is very cold ($T \sim 40$ K) and thus emits most of its radiation at longer wavelengths (80 to 100 μm and higher) than other solar system bodies observed to date. CH_4 and N_2 ice, both observed at Triton's surface, are relatively transparent compared to water ice, the predominant surface component on most other icy satellites [see, for example, Irvine and Pollack (*20*); Savoie and Fournier (*21*)]. Even water ice becomes significantly more transparent at Triton's longer thermal wavelengths (*20*). Therefore, the surface particles on Triton may not be as efficient emitters as those on other satellites, leading to the observed lower emissivity.

It should also be noted that we have assumed that insolation is the only significant heat source. Due to Triton's high Bond albedo and distance from the sun, its solar energy input is unusually low, and additional heat sources such as the decay of radionuclides in Triton's interior may provide additional heat on the order of 10% of the solar input (*22*), leading to a similar increase in the estimated emissivity.

REFERENCES AND NOTES

1. B. A. Smith *et al.*, *Science* **246**, 1422 (1989).
2. B. Hapke, *J. Geophys. Res.* **86**, 3039 (1981).
3. ———, *Icarus* **59**, 41 (1984).
4. ———, *ibid.* **67**, 264 (1986).
5. D. J. van Blerkom, *ibid.* **14**, 235 (1971).
6. S. Chandrasekhar, *Radiative Transfer* (Dover, New York, 1961).
7. J. D. Goguen, H. B. Hammel, R. H. Brown, *Icarus* 77, 239 (1989).
8. N. L. Lark, H. B. Hammel, D. P. Cruikshank, D. J. Tholen, M. A. Rigler, *ibid.* **79**, 15 (1989).
9. G. L. Tyler *et al.*, *Science* **246**, 1466 (1989); A. L. Broadfoot *et al.*, *ibid.*, p. 1459.
10. B. J. Buratti, *Icarus* **61**, 208 (1985).
11. J. Veverka, in *Planetary Satellites*, J. Burns, Ed. (Univ. of Arizona Press, Tucson, AZ, 1977), pp. 171–209.
12. H. Campins, G. H. Rieke, M. J. Lebofsky, *Astron. J.* **90**, 896 (1985).
13. A. Verbiscer and J. Veverka, *Bull. Am. Astron. Soc.* **20**, 872 (1988).
14. Taken from J. C. Arveson, R. N. Griffin, Jr., B. D. Pearson, Jr., *Appl. Opt.* **8**, 2215 (1969).
15. D. J. Tholen, referenced in Smith *et al.* (*1*).
16. D. P. Cruikshank and J. Apt, *Icarus* **58**, 306 (1984).
17. J. R. Spencer, M. W. Buie, G. L. Bjoraker, in preparation.
18. D. P. Cruikshank, R. H. Brown, A. T. Tokunaga, R. G. Smith, J. R. Piscitelli, *Icarus* **74**, 413 (1988).
19. J. Veverka, P. Thomas, T. V. Johnson, D. Matson, K. Housen, in *Satellites*, J. A. Burns, Ed. (Univ. of Arizona Press, Tucson, AZ, 1986).
20. W. M. Irvine and J. B. Pollack, *Icarus* **8**, 324 (1968).
21. R. Savoie and R. P. Fournier, *Chem. Phys. Lett.* 7, 1 (1970).
22. R. H. Brown, *Science* **250**, 431 (1990).

23. The authors thank R. Thompson for many helpful suggestions. This research was supported by the Voyager Project and by NASA grants NSG 7156 and NAGW-2084.

9 August 1990; accepted 14 September 1990

Surface and Airborne Evidence for Plumes and Winds on Triton

C. J. HANSEN, A. S. MCEWEN, A. P. INGERSOLL, R. J. TERRILE

Aeolian features on Triton that were imaged during the Voyager Mission have been grouped. The term "aeolian feature" is broadly defined as features produced by or blown by the wind, including surface and airborne materials. Observations of the latitudinal distributions of the features probably associated with current activity (known plumes, crescent streaks, fixed terminator clouds, and limb haze with overshoot) all occur from latitude −37° to latitude −62°. Likely indicators of previous activity (dark surface streaks) occur from latitude −5° to −70°, but are most abundant from −15° to −45°, generally north of currently active features. Those indicators which give information on wind direction and speed have been measured. Wind direction is a function of altitude. The predominant direction of the surface wind streaks is found to be between 40° and 80° measured clockwise from north. The average orientation of streaks in the northeast quadrant is 59°. Winds at 1- to 3-kilometer altitude are eastward, while those at >8 kilometers blow west.

THE VOYAGER 2 SPACECRAFT ACquired a series of high-resolution images of Triton on 25 and 26 August 1989. These images showed aeolian features, such as surface wind streaks, elongated clouds, and material from active plumes being carried downwind (*1*). The ultraviolet spectrometer detected a thin atmosphere whose dominant constituent is N_2 with a CH_4 mole fraction of 2.5×10^{-6} (*2*). The atmospheric pressure was determined by the refraction of Voyager's radio signal through Triton's atmosphere to be 1.6 ± 0.3 P (*3*). Triton's near-surface temperature was determined by Voyager's ultraviolet spectrometer and infrared detector (*2, 4*) to be ~38 K. A model for sublimation-driven winds was developed subsequently (*5*) to describe Triton's atmospheric circulation.

The aeolian features (that is, features produced by or blown by the wind including surface and airborne materials) revealed in Voyager Triton images have been categorized and analyzed to gain additional insight into Triton's atmospheric dynamics. The latitudinal distribution, direction, altitude, and length have been measured. The data set used consists of a total of 16 narrow angle frames and 1 wide angle frame [see Smith *et al.* (*6*) for a description of the camera optics] with resolutions ranging from 1.4 to 81 km per line pair. These images were acquired over a period of 2 days, during which the spacecraft flew over Triton's north pole and the phase angle changed from 38° to 159° to 133°.

Aeolian features are manifested in imaging data in different ways. This report categorizes these features by their morphology and the way in which they were detected rather than by source or process although inferences will be drawn with respect to source. The classification is done this way in order to clearly establish the reliability of any particular observation. Along with surface streaks and known eruption columns, we are describing other elongated clouds, some of which appear to have fixed sources on the surface and may be other eruptions. With this approach observations of aeolian features are categorized as (i) active plumes, (ii) surface wind streaks, (iii) terminator clouds, (iv) crescent streaks, (v) limb hazes, and (vi) bright rays.

The most dramatic observations of material carried by wind in Triton's atmosphere

C. Hansen and R. Terrile, Jet Propulsion Laboratory, Pasadena, CA 91109.
A. McEwen, U.S. Geological Survey, Flagstaff, AZ 86001.
A. Ingersoll, California Institute of Technology, Pasadena, CA 91125.

are the two geyser-like plumes discovered with stereo analysis by L. Soderblom [figure 38 of Smith *et al.* (*1*)]. These two plumes ("east plume" and "west plume") inject their contents into the atmosphere and are carried downwind over 100 km (*1*). A computer time-lapse sequence was developed to clearly show the shift of these two high plumes relative to the surface due to parallax (*7*). Visible in this sequence of the east plume are two other dark features which move with the same magnitude and direction as the "east plume." Although their source region is not as clearly identifiable as the "east plume," we consider them to also be eruptions reaching 8 km. The direction of the wind evidenced by the direction in which material is being carried is almost due west.

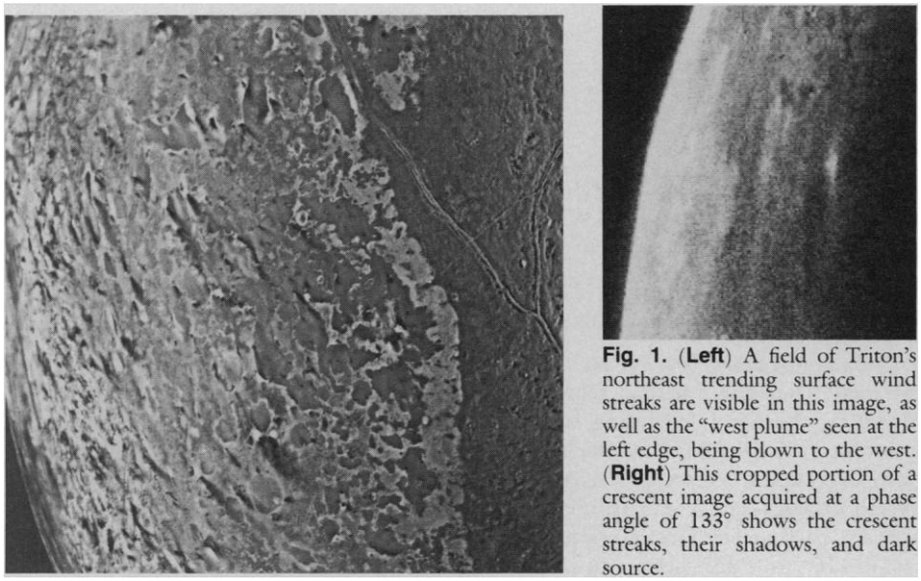

Fig. 1. (**Left**) A field of Triton's northeast trending surface wind streaks are visible in this image, as well as the "west plume" seen at the left edge, being blown to the west. (**Right**) This cropped portion of a crescent image acquired at a phase angle of 133° shows the crescent streaks, their shadows, and dark source.

Immediately obvious in the Voyager images were wind streaks, preferentially oriented northeast. Figure 1 (left) illustrates a field of surface wind streaks and also shows the "west plume." Generally, these features are fan-shaped with a dark narrow point and a more diffuse broad tail. The lengths and orientations for 119 of the streaks have been measured. Lengths of these streaks range from 4 to 117 km, with an average length of 26 km, but over half are between 5 and 20 km long. Determination of source and termination points for streaks is somewhat subjective. Conventions used for this analysis were that the source is the darkest (or brightest at high phase angles) point at the opening end of the "fan" and the termination is the furthest extent of the fan. In cases where the "fan" is only a straight line the orientation may be off 180°. In all cases of well-defined fans the angle over which mate-

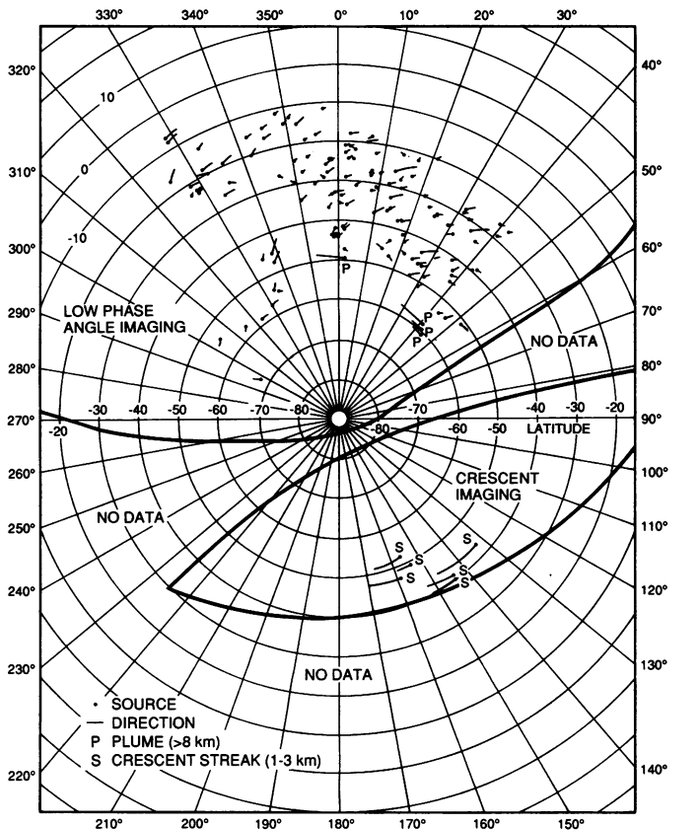

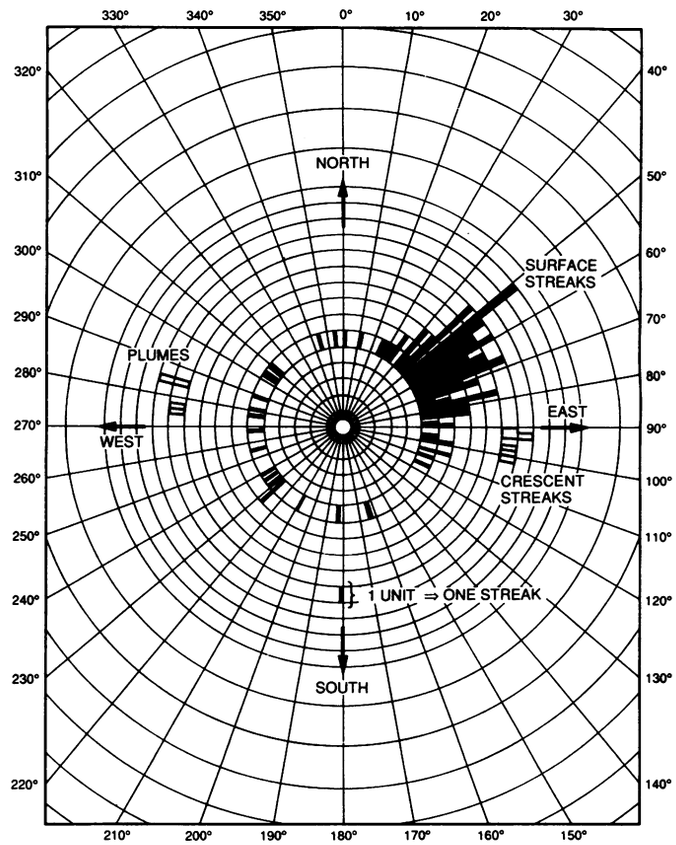

Fig. 2. (**Left**) This polar plot of Triton's southern hemisphere shows the geographic distribution of surface streaks, crescent streaks (1- to 3-km altitude), and eruption plumes (8-km altitude). The latitude and longitude of the feature source is plotted as a dot, while the "tail" shows both the length and direction of the streaks. Lower resolution coverage limited measurements of streaks in the longitude range 60° to 120° and 180° to 300° east. Terrain was visible up to 45° north latitude between 330° and 20° longitude but no streaks were detected north of −5° latitude. (**Right**) This modified rose diagram clearly shows the preferential orientation of aeolian features as a function of altitude. Eruption plumes are blown westward while crescent streaks at 1 to 3 km altitude are oriented eastward. Surface streaks predominantly point northeast.

rial has been strewn has been measured in order to gain more insight into the processes active in the Ekman layer.

Stereo analysis of the images showed the wind streaks to be on or very near (<1 km) the surface (*7*). The responsible process could be injection of material into the atmosphere and its subsequent settling out, or saltation of particles by the ambient Triton winds. These two possibilities have been analyzed by Sagan and Chyba (*8*) and they find that both are plausible.

The streaks are distributed in latitude from −5° to −70° but are most abundant from −15° to −45°, as can be seen in Fig. 2 (left). Orientations of wind streaks fall predominantly between 40° and 80° measured clockwise from north, as can be seen in Fig. 2 (right). Of the 95 streaks in this northeast quadrant the average direction is 59°. Surface wind streaks which are clearly oriented in a different direction could be indicative of material blown in a direction determined by the local topography. There are also other "source areas" present in the images which show material deposited on the surroundings but for which there is no clear orientation. We find no clear correlation of length or direction with latitude.

Crescent images of Triton revealed the presence of clouds along the terminator [figure 3b of Smith *et al.* (*1*)]. This material is high enough in the atmosphere to be illuminated although the underlying terrain is already in darkness. One very long cloud feature was observed to rotate with Triton. Minimum cloud altitude may be calculated from the incidence angle. This cloud's altitude of >13 km makes it clearly an atmospheric feature as opposed to a high mountain range. This terminator cloud is also probably due to one or more eruptions, but it is much higher and longer (>400 km) than the plumes observed at low phase angles. The nature of the observation prohibits being able to determine the cloud's orientation.

Another discrete cloud feature was identified on the terminator and was observed to move relative to the surface. For this feature we were able to measure both its altitude (>5 km) and wind velocity (approximately 13 m/s eastward). However, because this velocity is similar to the velocity of the terminator at this latitude, an alternative interpretation is that different parts of a stationary, elongated, east-west cloud are being illuminated. In this case the cloud is at least 380 km long.

Long bright streaks on the illuminated surface in crescent images, termed here "crescent streaks," were identified by Smith *et al.* [figure 37 in (*1*)] as atmospheric plumes, based on their morphology and on the assumption that the dark adjacent streaks are the shadows cast by these plumes. At least six east-west trending elongated clouds can be seen over the illuminated part of the surface in crescent images. Some of the clouds appear to cast shadows, which indicates that they are 1 to 3 km high. They appear most distinct at their western ends and become more diffuse and faint to the east, which suggests fixed sources relative to the surface and an eastward atmospheric motion. One of these clouds appears to begin from a dark surface feature, as can be seen in Fig. 1 (right). They are 77 to 254 km long and about 10 km wide and occur from latitude −40° to −51°. The lengths, widths, latitudinal distribution and east-west orientations of these clouds are similar to the active plumes. They differ from the active plumes in altitude (1 to 3 km versus 8 km), direction of motion (eastward versus westward), and brightness relative to the surface (bright versus dark, perhaps due to phase angle).

Optically thin and optically thick limb hazes were observed and reported by Smith *et al.* [figure 34 in (*1*)]. The discrete optically thick hazes are for the most part only observed obliquely but in one case the haze on the limb shows the overshoot characteristic of the plumes, has a westward direction from the presumed source and an altitude of at least 6.5 km, and thus has been added to the data set as an active eruption. Because of the viewing geometry it is not possible to establish a length or direction for these hazes but they are discrete, separated from the surface, and are not ubiquitous.

A bright fringe and north-trending rays are associated with Triton's south polar cap (*9*) (Fig. 3). The fringe and rays appear diffusely deposited over both the south polar cap and the relatively dark areas to the north. The cap margin shows a pattern of "scallops," each about 20° wide and the bright rays emanate preferentially from the points of the scalloped margin. These bright rays extend north-northeast for hundreds of kilometers. Spectral properties of the fringe are consistent with those of fresh frost or snow, suggesting that these rays could consist of fine-grained frost or snow that has been entrained by northward, Coriolis-deflected winds.

Figure 2 (left) shows a plot in polar coordinates of the locations, lengths, and directions of the plumes, surface wind streaks, and crescent streaks. This is not a complete inventory in the sense that measurements are limited by the viewing geometry and resolution as a function of time. Resolution was insufficient to detect wind streaks as anything more than dark features prior to 5 hours before closest approach to Triton. Crescent streaks and terminator clouds were only detectable for about 2 days following closest approach. Boundaries of terrain available for measurements (that is, not constrained by the viewing geometry) are marked on the figure.

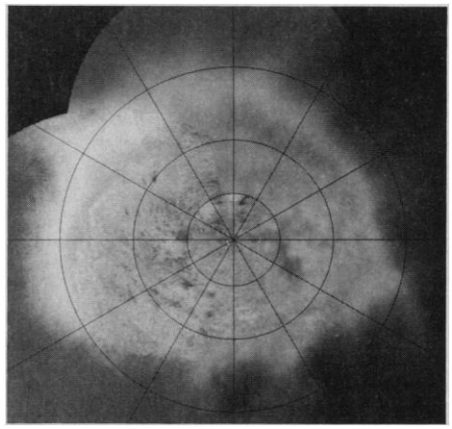

Fig. 3. Bright rays are seen to emanate from the boundaries of the bright fringe. Their northeast orientation in the northern hemisphere is consistent with winds blowing from south to north and being deflected by the Coriolis force.

Figure 2 (right) is a modified rose diagram showing the wind direction illustrated by the orientation of these features. It is immediately apparent that there is a preferred orientation for the surface wind streaks, crescent streaks, and active plumes, and that these preferred orientations differ. The near surface winds are predominantly between 40° and 80° measured clockwise from north. The crescent streaks point southeast, while the material from active eruptions is carried west. The key to understanding this phenomena is in noting that they are all at different altitudes. The surface streaks are on or near the surface, the crescent streaks are 1 to 3 km above the surface, and the active plumes are blown westward at an altitude of 8 km.

Ingersoll (*5*) explains the direction of surface streaks as the result of Ekman layer outflow from the subliming polar cap. The northeastward direction of the surface streaks and bright rays agrees with the direction of the surface stress in the model, implying that they are controlled by the wind close to the ground. The model predicts an eastward geostrophic wind just above the Ekman layer, whose thickness Ingersoll estimates as 1 km. This prediction is borne out by the present work, in which eastward-trending crescent streaks at 1- to 3-km altitude were observed. The wind apparently reverses direction at higher altitudes. The fact that the plumes blow to the west at 8-km altitude is attributed by Ingersoll to an equator-to-pole temperature gradient in the atmosphere. That is, according to the ther-

Table 1. Atmospheric features probably attributable to current activity.

Feature	From latitude	Longitude	To latitude	Longitude
West plume	−49°	2°	−49°	352°
East plume	−57°	41°	−56°	27°
East plume companion 1	−59°	43°	−59°	36°
East plume companion 2	−60°	44°	−60°	37°
Limb haze with overshoot	−62°	67°	−69°	37°
Terminator cloud (fixed)	−37°	313°	−30°	337°
Crescent streak 1	−40°	144°	−40°	152°
Crescent streak 2	−41°	144°	−42°	152°
Crescent streak 3	−43°	133°	−44°	148°
Crescent streak 4	−47°	159°	−47°	170°
Crescent streak 5	−49°	154°	−49°	159°
Crescent streak 6	−51°	156°	−52°	167°

mal wind equation, the atmosphere over the equator must be warmer than that over the southern pole.

The surface stress in a laminar Ekman layer is exactly 45° to the left of the geostrophic wind (45° clockwise from north). The surface stress in a turbulent Ekman layer is closer to the direction of the geostrophic wind (*5*). One interpretation of our result, that the streaks are oriented predominantly 40° to 80° clockwise from north, is that the Ekman layer is turbulent. This interpretation is consistent with Ingersoll (*5*), who estimates that the eddy viscosity K is about 10 m^2 s^{-1}, several hundred times the molecular viscosity. Another interpretation is that the streaks are controlled by the wind slightly above the surface in a laminar Ekman layer. In this case streak orientation may be used to derive the material's altitude.

A major unknown is the thermal stratification of the atmosphere. If further analysis of the Voyager radio science, infrared, and ultraviolet spectrometer data were to give an improved temperature profile, then the level of turbulence and altitude of the streak material could be inferred from our data.

The latitudinal distribution of aeolian features is important evidence that plume activity is controlled by the seasonal migration of the subsolar latitude on Triton. Triton's subsolar latitude in 1989 was −45° while 10 years ago it was −35°. Maximum diurnal insolation occurs at the south pole, but subsurface temperatures may lag behind surface temperatures. This evidence, presented in more complete form here than elsewhere, is the basis for the assumption that the plumes are powered by solar energy. One possible explanation is that they are at least partially driven by greenhouse nitrogen (*7, 11*). Table 1 lists atmospheric features which are probably due to current eruptive activity. If this is the case, at least 12 eruptions are occurring on Triton simultaneously.

REFERENCES AND NOTES

1. B. Smith *et al.*, *Science* **246**, 1422 (1989).
2. L. Broadfoot *et al.*, *ibid.*, p. 1459.
3. G. Tyler *et al.*, *ibid.*, p. 1466.
4. B. Conrath *et al.*, *ibid.*, p. 1454.
5. A. Ingersoll, *Nature* **344**, 315 (1990).
6. B. Smith *et al.*, *Space Sci. Rev.* **21**, 103 (1977).
7. L. Soderblom *et al.*, *Science* **250**, 410 (1990).
8. C. Sagan, *Nature* **346**, 546 (1990).
9. A. McEwen *et al.*, *Geophys. Res. Lett.* **17**, 1765 (1990).
10. The locations and orientations of all aeolian features were measured using raw images and both VICAR and PICS image processing software. A cursor was placed at the source and termination of all wind streaks, plumes, and so on, and line and sample of the cursor was retrieved. Lines and samples of points measured were converted to latitude and longitude on a 1350-km radius Triton using the NAIF (Navigation Ancillary Information Facility at JPL) OLSEDR (Online Supplementary Experiment Data Record) program. From latitude and longitude both length and direction may be computed. A total of 132 features have been measured.
11. R. Brown *et al.*, *Science* **250**, 431 (1990).

12. This research was carried out by the Jet Propulsion Laboratory, California Institute of Technology, under a contract with the National Aeronautics and Space Administration. The authors thank the Voyager Flight Team for their careful implementation of a complicated imaging observation.

9 August 1990; accepted 24 September 1990

Subsurface Energy Storage and Transport for Solar-Powered Geysers on Triton

RANDOLPH L. KIRK, ROBERT H. BROWN, LAURENCE A. SODERBLOM

The location of active geyser-like eruptions and related features close to the current subsolar latitude on Triton suggests a solar energy source for these phenomena. Solid-state greenhouse calculations have shown that sunlight can generate substantially elevated subsurface temperatures. A variety of models for the storage of solar energy in a sub-greenhouse layer and for the supply of gas and energy to a geyser are examined. "Leaky greenhouse" models with only vertical gas transport are inconsistent with the observed upper limit on geyser radius of ~1.5 kilometers. However, lateral transport of energy by gas flow in a porous N_2 layer with a block size on the order of a meter can supply the required amount of gas to a source region ~1 kilometer in radius. The decline of gas output to steady state may occur over a period comparable with the inferred active geyser lifetime of five Earth years. The required subsurface permeability may be maintained by thermal fracturing of the residual N_2 polar cap. A lower limit on geyser source radius of ~50 to 100 meters predicted by a theory of negatively buoyant jets is not readily attained.

A HIGHLIGHT OF THE VOYAGER 2 encounter with Triton was the discovery of geyser-like plumes in the atmosphere, along with clouds and surface deposits (streaks) that may be related to the plumes in origin (*1–3*). The proximity of these features to the current subsolar latitude prompted the suggestion that the plumes are powered (or at least in some way triggered) by insolation. Smith *et al.* (*1*) outlined an insolation-driven geyser model in which sunlight is absorbed at the base of a "solid-state greenhouse" layer of clear nitrogen ice, increasing the subsurface temperature and creating a reservoir of high-pressure gas to feed the geyser in the pore space beneath. Subsequent calculations by Brown *et al.* (*4*) have confirmed that temperatures substantially (degrees or even tens of degrees) above ambient can be generated either in a thin, transparent "super greenhouse" layer underlain by a dark absorber or in a deeper, translucent "classical greenhouse."

The purpose of this report is to explore a range of models of the subsurface "plumbing" of an insolation-driven geyser: the processes by which absorbed solar energy is stored, transmitted, and released to supply nitrogen gas to the plume. Focusing on subsurface processes, we treat both the greenhouse layer and the erupting plume approximately, as simplified boundary conditions, rather than model them in detail. We attempt to construct models that can account for the observed and deduced properties of the geysers and to answer some of